JOURNAL OF SOLID STATE CHEMISTRY **122,** 15–21 (1996)
ARTICLE NO. 0074

Crystal Structures and Characterization of $Ca_9Fe(PO_4)_7$ and $Ca_9FeH_{0.9}(PO_4)_7$

B. I. Lazoryak,* V. A. Morozov, and A. A. Belik

Chemical Department, Moscow State University, 119899, Moscow, Russia

and

S. S. Khasanov and V. Sh. Shekhtman

Institute of Solid State Physics, Russian Academy of Sciences, 142452, Chernogolovka, Russia

Received February 22, 1995; in revised form October 18, 1995; accepted October 24, 1995

Whitlockite-like compounds s- and o-$Ca_9Fe(PO_4)_7$ and r-$Ca_9FeH_{0.9}(PO_4)_7$ were prepared and studied by XRD, IR, Mössbauer technique, and diffuse reflective spectroscopy. The crystal structures of the three phases were determined by the Rietveld analysis. The unit cell is hexagonal with $a = 10.3391(2)$ Å, $c = 37.130(1)$ Å, s-$Ca_9Fe(PO_4)_7$; $a = 10.3543(2)$ Å, $c = 37.168(1)$ Å, r-$Ca_9FeH_{0.9}(PO_4)_7$; and $a = 10.3406(2)$ Å, $c = 37.157(1)$ Å, o-$Ca_9Fe(PO_4)_7$; $Z = 6$; $R3c$ space group. The redox reactions proceed reversibly without destruction of the crystal lattice in double calcium–iron phosphates and the oxygen stoichiometry is not variable. The introduction of hydrogen into the lattice causes a change of the P(1)–O(11) bond length and the formation of an O(11)–H ... O(34) hydrogen bond. The redox reactions are accompanied by a position change of oxygen atoms O(24) and O(33). The main differences between the three phases are discussed on the basis of the crystal structures.

1. INTRODUCTION

The present work is the second part of our investigation of the redox reaction in double calcium–iron phosphate. Previously it was found (1) that in double calcium–iron phosphates the redox reactions proceed reversibly without destruction of the crystal lattice according to the equations

$$Ca_9Fe^{3+}(PO_4)_7 + 0.45H_2 = Ca_9Fe^{2+}_{0.9}Fe^{3+}_{0.1}H_{0.9}(PO_4)_7 \quad [I]$$

$$Ca_9Fe^{2+}_{0.9}Fe^{3+}_{0.1}H_{0.9}(PO_4)_7 + 0.225O_2 = Ca_9Fe^{3+}(PO_4)_7 + 0.45H_2O. \quad [II]$$

* To whom correspondence should be addressed.

Such kinds of reactions occur in double phosphates $Ca_{19}Ce(PO_4)_{14}$ (2), $Ca_{19}Cu(PO_4)_{14}$ (3), and $Ca_{3-y}Ni_y(XO_4)_2$ (X = P, As) (4, 5). These compounds belong to the whitlockite-like ($Ca_{18.19}Mg_{1.17}Fe_{0.83}H_{1.62}(PO_4)_{14}$ (6)) structural family and exhibit interesting solid-state properties. Calcium–nickel phosphate is used industrially to obtain butadiene from butenes (4, 5). Compounds with iron, copper, or cerium can be used as materials for fossil energy conversion (7) and sensor materials (3). Structures of such compounds have not been studied yet.

In this paper we describe the structures of s-$Ca_9Fe(PO_4)_7$ (as-synthesized phase), r-$Ca_9FeH_{0.9}(PO_4)_7$ (reduced phase), and o-$Ca_9Fe(PO_4)_7$ (oxidized phase) and discuss the difference between them. The study of their crystal structures allows us to promote understanding of the mechanism of the reversible redox reactions in solid state.

2. EXPERIMENTAL

s-$Ca_9Fe(PO_4)_7$ compound was synthesized according to the equation $9CaCO_3 + 0.5Fe_2O_3 + 7NH_4H_2PO_4 = Ca_9Fe(PO_4)_7 + 9CO_2 + 7NH_3 + 10.5H_2O$ [III] by heating at 573 K for 5 h and at 1370 K for 40 h in a platinum crucible in air. Several cycles of heating and grinding were necessary to complete the solid-state reaction at 1370 K. The chemical analysis showed that the composition was close to the theoretical value corresponding to $Ca_9Fe(PO_4)_7$. The results were as follows: Ca = 46.68%, Fe = 7.37%, and P_2O_5 = 45.95% (theoretically, Ca = 46.5%, Fe = 7.4%, and P_2O_5 = 46.1%). The obtained powder was red.

The experimental X-ray powder diffraction data for structural refinements of the three phases were collected by using one and the same sample which was prepared under different conditions:

0022-4596/96 $18.00

TABLE 1
Crystallographic Data, Recording Conditions, and Refinement Results of Double Calcium–Iron Phosphates

	s-$Ca_9Fe(PO_4)_7$	r-$Ca_9FeH_{0.9}(PO_4)_7$	o-$Ca_9Fe(PO_4)_7$
Space group	*R*3*c*	*R*3*c*	*R*3*c*
2Θ range(°)	10–140	10–140	10–140
Step scan increment (2Θ)	0.01	0.01	0.01
I_{max}	35000	35000	35500
Unit-cell parameters			
a (Å),	10.3391(2)	10.3543(2)	10.3406(2)
c (Å),	37.130(1)	37.168(1)	37.157(1)
V (Å^3),	3432(1)	3450(2)	3441(2)
Z	6	6	6
Number of reflections	807	807	807
Number of refined parameters			
with refined B_{iso}	70	70	70
with fixed B_{iso}	53	53	53
Profile function (psuedo-Voight, η)	0.371(4)	0.501(3)	0.418(5)
Profile parameters			
U	0.135(2)	0.0691(2)	0.0793(3)
V	0.0874(9)	0.0696(5)	0.0784(7)
W	0.0384(3)	0.0319(4)	0.0392(5)
Reliable factors[a]			
R_{WP}	3.77	3.69	3.54
	3.85[b]	3.85[b]	3.66[b]
R_P	2.81	2.81	2.66
	2.95[b]	2.97[b]	2.80[b]
R_I	4.21	2.45	2.48
	4.48[b]	3.03[b]	3.09[b]
R_F	2.80	2.33	2.44
	3.02[b]	2.91[b]	2.06[b]

[a] Defined as follows: $R_{WP} = [(\Sigma W_i [Y_{obs} - Y_{cal}]^2/(\Sigma W_i [Y_{obs}]^2)]^{1/2}$, $R_P = (\Sigma|Y_{obs} - Y_{cal}|)/(\Sigma Y_{obs})$, $R_I = (\Sigma|I_{obs} - I_{cal}|)/(\Sigma I_{obs})$, $R_F = (\Sigma|[I_{obs}]^{1/2}|) - [I_{cal}]^{1/2}/(\Sigma [I_{obs}]^{1/2})$.
[b] Results of refinement with fixed B_{iso}.

1. The first X-ray pattern was carried out on a red sample of s-$Ca_9Fe(PO_4)_7$ obtained according to Eq. [III].

2. s-$Ca_9Fe(PO_4)_7$ was reduced in the mixture of 90%Ar + 10%H_2 at 800 K for 5 h according to Eq. [I] and then cooled in the same atmosphere, and X-ray powder diffraction data were collected. The obtained powder of r-$Ca_9FeH_{0.9}(PO_4)_7$ was white-grayish.

3. r-$Ca_9FeH_{0.9}(PO_4)_7$ was oxidized in air at 1300 K for 24 h according to Eq. [II] and X-ray patterns were recorded. The obtained powder of o-$Ca_9Fe(PO_4)_7$ was red.

X-ray powder diffraction (XRD) patterns were taken at room temperature by using a diffractometer SIEMENS D500 (Cu$K_{\alpha 1}$ radiation (λ = 1.540598 Å), SiO_2 monochromator) in the range 2Θ = 10°–140° with a step of 0.01°. IR spectra were recorded on a Perkin–Elmer spectrophotometer in the range 400–4000 cm^{-1} using KBr-pellet technique. Mössbauer spectra were recorded in transmission geometry applying usual techniques (constant acceleration signal spectrometer with a ^{57}Co source diffused into a copper matrix). Diffuse reflective spectra were recorded at room temperature on Spectroton spectrophotometer in the range of 380 to 720 nm.

3. RESULTS

s-$Ca_9Fe(PO_4)_7$, r-$Ca_9FeH_{0.9}(PO_4)_7$, and o-$Ca_9Fe(PO_4)_7$ obtained under different conditions were single-phased. Their X-ray diffraction patterns were similar to whitlockite-like compounds (8–12). The X-ray diffraction patterns of samples were indexed in a hexagonal unit cell with the *R*3*c* space group. Intensities and *d*-spacing for s-$Ca_9Fe(PO_4)_7$ and r-$Ca_9FeH_{0.9}(PO_4)_7$ are listed in Powder Diffraction Files 45-338 and 45-553. The experimental density found by pycnometer in benzene for s-$Ca_9Fe(PO_4)_7$ is 3.10(2) g/cm^3, which is close to the theoretical value of 3.14 g/cm^3 for six $Ca_9Fe(PO_4)_7$ formula units per unit cell.

The structures of s- and o-$Ca_9Fe(PO_4)_7$, and r-$Ca_9FeH_{0.9}(PO_4)_7$ were refined from X-ray powder data using the Rietveld technique (13). The crystallographic charac-

TABLE 2
Fractional Atomic Coordinates and Thermal Parameters for Double Calcium–Iron Phosphates

Atom	Phase[a]	x	y	z	B_{iso}
Ca(1)	s	0.719(1)	0.852(2)	0.4337(5)	0.2(2)
	r	0.722(1)	0.852(1)	0.4352(6)	0.3(2)
	o	0.7204(9)	0.854(2)	0.4344(5)	0.5(2)
Ca(2)	s	0.622(1)	0.824(2)	0.2331(5)	1.2(2)
	r	0.618(1)	0.821(1)	0.2332(6)	1.0(2)
	o	0.6220(9)	0.825(2)	0.2335(5)	1.1(2)
Ca(3)	s	0.127(1)	0.2750(7)	0.3271(5)	0.5(2)
	r	0.128(1)	0.2806(8)	0.3284(5)	1.5(2)
	o	0.128(1)	0.2749(7)	0.3275(5)	0.7(2)
Fe	s	0.0	0.0	0.0	0.5(2)
	r	0.0	0.0	0.0	0.7(2)
	o	0.0	0.0	0.0	0.8(2)
P(1)	s	0.0	0.0	0.2713(6)	0.9(4)
	r	0.0	0.0	0.2642(8)	3.2(6)
	o	0.0	0.0	0.2712(6)	1.4(4)
P(2)	s	0.684(1)	0.853(2)	0.1371(5)	0.2(3)
	r	0.681(1)	0.848(2)	0.1361(5)	0.3(2)[b]
	o	0.683(1)	0.852(2)	0.1376(5)	0.2(2)
P(3)	s	0.656(2)	0.850(2)	0.0328(6)	1.8(4)
	r	0.646(2)	0.848(2)	0.0332(6)	1.3(4)
	o	0.655(2)	0.850(2)	0.0332(5)	1.5(3)
O(11)	s	0.0	0.0	0.3148(9)	2.4(8)[b]
	r	0.0	0.0	0.3101(9)	2.1(6)[b]
	o	0.0	0.0	0.3131(8)	2.0(6)[b]
O(12)	s	0.017(3)	0.867(2)	0.2580(9)	0.4(6)
	r	0.025(3)	0.868(2)	0.2591(9)	1.0(7)
	o	0.018(2)	0.868(2)	0.2592(9)	0.0(5)
O(21)	s	0.729(3)	0.913(3)	0.1753(9)	1.8(8)
	r	0.728(3)	0.911(4)	0.1780(9)	1.2(8)
	o	0.729(3)	0.912(3)	0.1759(9)	1.8(8)
O(22)	s	0.743(4)	0.758(4)	0.1240(8)	1.5(9)
	r	0.745(4)	0.762(4)	0.1230(8)	1.4(9)
	o	0.745(4)	0.760(4)	0.1233(9)	1.5(9)
O(23)	s	0.722(4)	0.005(3)	0.1148(9)	0.2(7)
	r	0.724(4)	0.011(3)	0.1161(9)	1.1(8)
	o	0.723(3)	0.005(3)	0.1158(8)	2.5(6)[b]
O(24)	s	0.509(3)	0.761(5)	0.1352(9)	0.7(6)
	r	0.517(3)	0.758(4)	0.1320(9)	0.3(6)
	o	0.507(3)	0.758(4)	0.1350(9)	0.5(5)
O(31)	s	0.610(3)	0.946(3)	0.0470(8)	2.5(6)[b]
	r	0.609(3)	0.942(3)	0.0485(9)	1.3(6)[b]
	o	0.612(3)	0.948(3)	0.0476(9)	2.0(6)
O(32)	s	0.578(3)	0.693(3)	0.0524(9)	2.5(6)
	r	0.568(3)	0.689(3)	0.0549(9)	1.6(6)
	o	0.579(3)	0.695(3)	0.0530(8)	2.4(5)[b]
O(33)	s	0.824(3)	0.918(4)	0.0397(8)	2.5(6)
	r	0.827(3)	0.925(4)	0.0401(7)	1.3(8)
	o	0.825(3)	0.918(4)	0.0403(7)	2.4(5)[b]
O(34)	s	0.622(2)	0.813(4)	0.9923(9)	1.1(5)
	r	0.612(3)	0.812(4)	0.9930(9)	2.6(7)
	o	0.624(2)	0.817(4)	0.9928(8)	1.0(5)

[a] s-$Ca_9Fe(PO_4)_7$; r-$Ca_9FeH_{0.9}(PO_4)_7$; o-$Ca_9Fe(PO_4)_7$.
[b] Fixed $B_{iso.}$

TABLE 3
Interatomic Distances (Å) in Double Calcium–Iron Phosphates

Distance	s-$Ca_9Fe(PO_4)_7$	r-$Ca_9FeH_{0.9}(PO_4)_7$	o-$Ca_9Fe(PO_4)_7$
Ca(1)–O(12)	2.40(4)	2.42(2)	2.43(3)
–O(22)	2.68(4)	2.68(4)	2.70(4)
–O(23)	2.46(4)	2.48(4)	2.47(4)
–O(24)	2.57(4)	2.41(4)	2.53(4)
–O′(24)	2.53(4)	2.53(4)	2.52(4)
–O(31)	2.47(4)	2.50(4)	2.48(3)
–O(32)	2.29(3)	2.22(3)	2.31(3)
–O(34)	2.35(2)	2.36(2)	2.34(2)
Ca(2)–O(12)	2.29(3)	2.28(3)	2.29(3)
–O(21)	2.38(3)	2.35(3)	2.37(3)
–O(22)	2.51(2)	2.48(3)	2.45(3)
–O(23)	2.37(3)	2.37(3)	2.39(3)
–O(31)	2.58(3)	2.58(3)	2.56(3)
–O(32)	2.73(3)	2.78(2)	2.69(4)
–O(33)	2.49(4)	2.40(4)	2.50(4)
–O′(33)	2.45(2)	2.48(2)	2.47(3)
Ca(3)–O(11)	2.51(3)	2.61(1)	2.52(1)
–O(21)	2.61(2)	2.58(2)	2.63(2)
–O(22)	2.45(3)	2.49(2)	2.45(3)
–O(23)	2.35(3)	2.29(3)	2.35(3)
–O(31)	2.51(4)	2.52(3)	2.50(3)
–O(32)	2.58(3)	2.60(3)	2.60(3)
–O(34)	2.60(3)	2.56(3)	2.57(3)
–O′(34)	2.45(3)	2.46(4)	2.50(3)
Fe–O(33)*3	2.16(3)	2.16(4)	2.17(3)
–O(24)*3	1.96(3)	2.08(3)	1.95(3)
O(24)–O(24)*3	2.73(4)	2.85(6)	2.70(4)
O(33)–O(33)*3	2.73(5)	2.75(3)	2.71(5)
P(1)–O(11)	1.62(4)	1.71(4)	1.56(3)
–O(12)*3	1.55(2)	1.52(2)	1.54(2)
O(11)–O(12)*3	2.58(4)	2.43(4)	2.48(4)
O(12)–O(12)*3	2.55(4)	2.62(4)	2.55(4)
P(2)–O(21)	1.52(3)	1.62(3)	1.53(3)
–O(22)	1.48(3)	1.44(3)	1.49(3)
–O(23)	1.64(3)	1.69(3)	1.63(3)
–O(24)	1.57(2)	1.48(3)	1.57(3)
P(3)–O(31)	1.41(4)	1.34(4)	1.39(3)
–O(32)	1.59(3)	1.63(3)	1.58(4)
–O(33)	1.54(3)	1.65(3)	1.56(4)
–O(34)	1.55(3)	1.54(3)	1.54(4)
O(11)–O(34)	2.61(2)	2.57(3)	2.65(3)

teristics and the conditions of the diffraction experiments for the three phases are summarized in Table 1. The coordinates of atoms in the β-$Ca_3(PO_4)_2$ structure (10) were used as the starting coordinates for the structure refinements. The Rietveld refinement was made using the RIETAN program (14). The final values of the atomic and thermal parameters are listed in Table 2. Table 3 presents the interatomic distances.

Using Mössbauer spectroscopy it was determined that s- and o-$Ca_9Fe(PO_4)_7$ only contained Fe^{3+} cations while phase r-$Ca_9FeH_{0.9}(PO_4)_7$ contained 90%Fe^{2+} and 10%Fe^{3+}. Thus, the composition of the reduced phase (r) corresponds to the formula $Ca_9Fe^{2+}_{0.9}Fe^{3+}_{0.1}H_{0.9}(PO_4)_7$ and the composition of the s- and o-phases corresponds to $Ca_9Fe^{3+}(PO_4)_7$. The ratio Fe^{2+}/Fe^{3+} in r-$Ca_9FeH_{0.9}(PO_4)_7$ did not change after 2 h heating at 770 K in the mixture of 90%Ar + 10%H_2. Oxidation of r-$Ca_9FeH_{0.9}(PO_4)_7$ was completed in 20 min at 900 K in air.

The redox reactions are accompanied by a change of color in the compounds. The diffuse reflective spectra of s- and o-$Ca_9Fe(PO_4)_7$, and r-$Ca_9FeH_{0.9}(PO_4)_7$ are presented in Fig. 1. The colors of s- and o-$Ca_9Fe(PO_4)_7$ are slightly different, but the profiles of both spectra are the same in the region 380–720 nm. The color of o-$Ca_9Fe(PO_4)_7$ does not return to the color of s-$Ca_9Fe(PO_4)_7$ after 100 h heating at 1300 K. These data show that o-$Ca_9Fe(PO_4)_7$ does not return to s-$Ca_9Fe(PO_4)_7$. However, the color of the sample oxidized after reduction (o-$Ca_9Fe(PO_4)_7$) does not change after the first redox cycle.

Figure 2 shows the IR spectra of s-$Ca_9Fe(PO_4)_7$, o-$Ca_9Fe(PO_4)_7$, and r-$Ca_9FeH_{0.9}(PO_4)_7$. The absorption bands are observed in the range 400–1200 cm^{-1} which are characteristic of whitlockite-like orthophosphates (15, 16). More vibration modes become active because the PO_4^{3-} local symmetry is distorted and descends to C_1 and therefore a splitting of ν_3 vibration appears. The IR spectra of s- and o-$Ca_9Fe(PO_4)_7$ show identical features in the region 400–1200 cm^{-1}. The number of absorption bands and the intensity of bands in this region are the same for s- and o-$Ca_9Fe(PO_4)_7$, while the IR spectrum of r-$Ca_9FeH_{0.9}(PO_4)_7$ is different from the corresponding spectra of s- and o-$Ca_9Fe(PO_4)_7$ (Fig. 2).

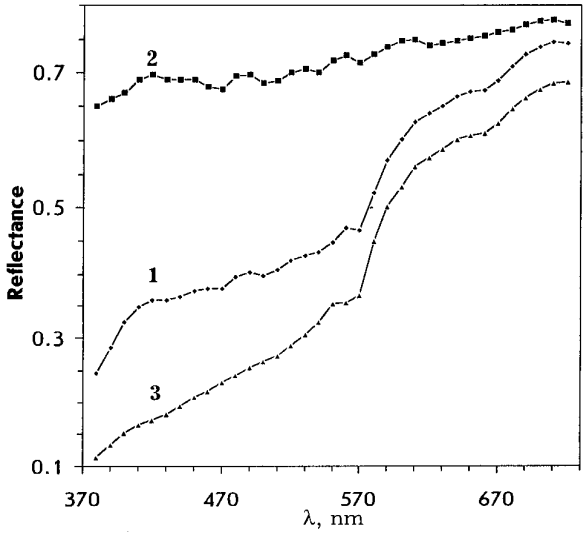

FIG. 1. Diffuse reflective spectra of double calcium–iron phosphates. (1) s-$Ca_9Fe(PO_4)_7$; (2) r-$Ca_9FeH_{0.9}(PO_4)_7$; and (3) o-$Ca_9Fe(PO_4)_7$.

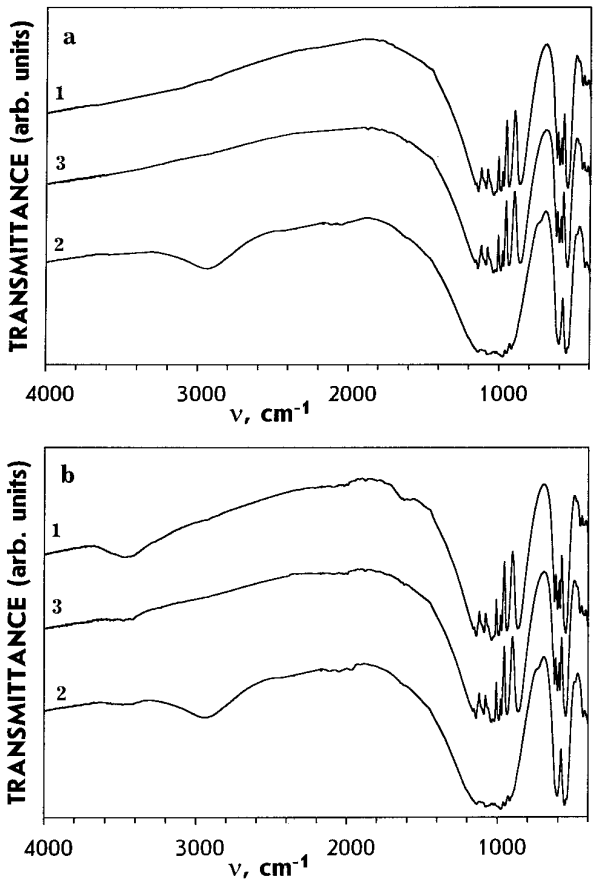

FIG. 2. IR spectra of double calcium–iron phosphates. (1) s-$Ca_9Fe(PO_4)_7$; (2) r-$Ca_9FeH_{0.9}(PO_4)_7$; and (3) o-$Ca_9Fe(PO_4)_7$. (a) Samples cooled in a dry box; (b) samples cooled in air.

Infrared spectrometric investigation shows that the reduction reaction is accompanied by the introduction of protons into the lattice. The proton-related hydroxyls are observed in the region of 2920 cm^{-1} for r-$Ca_9FeH_{0.9}(PO_4)_7$, but are not observed for s- and o-$Ca_9Fe(PO_4)_7$ (Fig. 2a). IR spectra of these three phases shown in Fig. 2a can be obtained only on samples cooled in a dry box. When s- and o-$Ca_9Fe(PO_4)_7$ are in contact with air, a band of absorption appears in the region of 3470 cm^{-1} of IR spectra (Fig. 2b) which apparently characterizes OH^- groups of adsorption water. s- and o-$Ca_9Fe(PO_4)_7$ phases adsorb very little quantity of water, which is not possible to detect with thermogravimetry.

4. DISCUSSION

The X-ray diffraction patterns of phases s- and o-$Ca_9Fe(PO_4)_7$, and r-$Ca_9FeH_{0.9}(PO_4)_7$ are very similar to each other (Fig. 3). The positions of peaks in the X-ray diffraction patterns show that o-$Ca_9Fe(PO_4)_7$ is intermediate between the s-$Ca_9Fe(PO_4)_7$ and r-$Ca_9FeH_{0.9}(PO_4)_7$ phases. These data as well as the data on diffuse reflective spectra prove that o-$Ca_9Fe(PO_4)_7$ does not return to s-$Ca_9Fe(PO_4)_7$. The intensities of some peaks change while passing from s(o)-$Ca_9Fe(PO_4)_7$ to r-$Ca_9FeH_{0.9}(PO_4)_7$ in the X-ray patterns. For example, peaks with Miller indices *1 2 2, 1 1 12,* and *3 1 2* are practically the same for s- and o-$Ca_9Fe(PO_4)_7$ but they are noticeably different from those for r-$Ca_9FeH_{0.9}(PO_4)_7$ (Fig. 3). It indicates that the introduction of protons into the lattice or their removal from the lattice causes small displacements of atoms. Such displacements are not enough for the destruction of the crystal lattice. The values of FWHM slightly increases while passing from s-$Ca_9Fe(PO_4)_7$ to r-$Ca_9FeH_{0.9}(PO_4)_7$ and come back to the initial values while passing from r-$Ca_9FeH_{0.9}(PO_4)_7$ to o-$Ca_9Fe(PO_4)_7$. For example, some peaks in different ranges 2Θ had the following FWHM: *1, 1, 2,* 0.11 (s), 0.12 (r), 0.11 (o); *0 2 10,* 0.11 (s), 0.12 (r), 0.11 (o); *1 4 6,* 0.12 (s), 0.14 (r), 0.13 (o); and *2 4 10,* 0.14 (s), 0.16 (r), 0.14 (o). The values of FWHM do not change with the accumulation of redox cycles. For example, the values of FWHM did not change even after more than 50 redox cycles. Their slight increase while passing from s-$Ca_9Fe(PO_4)_7$ to r-$Ca_9FeH_{0.9}(PO_4)_7$ is caused by microstress in crystals.

The structures of s- and o-$Ca_9Fe(PO_4)_7$ are very similar to each other and slightly different from the structure of r-$Ca_9FeH_{0.9}(PO_4)_7$. The structures of these three phases are similar to $Ca_{18}Mg_2H_2(PO_4)_{14}$ (8), $Ca_{18}Mn_2H_2(PO_4)_{14}$ (9), β-$Ca_3(PO_4)_2$ (10), $Ca_{3-x}Mg_x(PO_4)_2$ ($x = 0.11, 0.29$) (11), and mineral whitlockite $Ca_{18.19}(Mg_{1.17}Fe_{0.83})H_{1.62}(PO_4)_{14}$

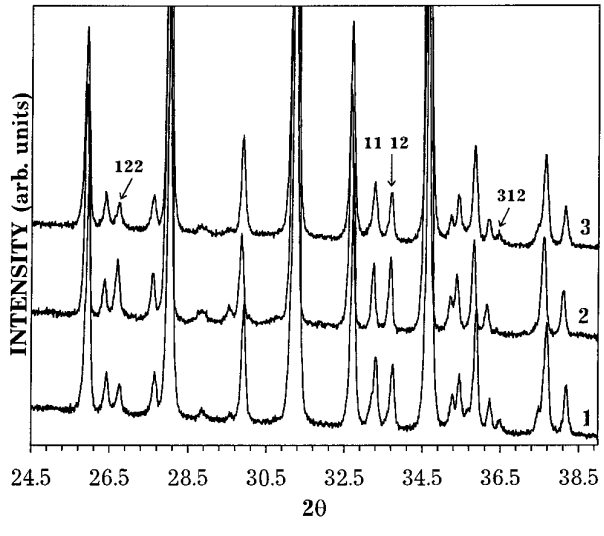

FIG. 3. A fragment of observed X-ray powder diffraction patterns for double calcium–iron phosphates. (1) s-$Ca_9Fe(PO_4)_7$; (2) r-$Ca_9FeH_{0.9}(PO_4)_7$; and (3) o-$Ca_9Fe(PO_4)_7$.

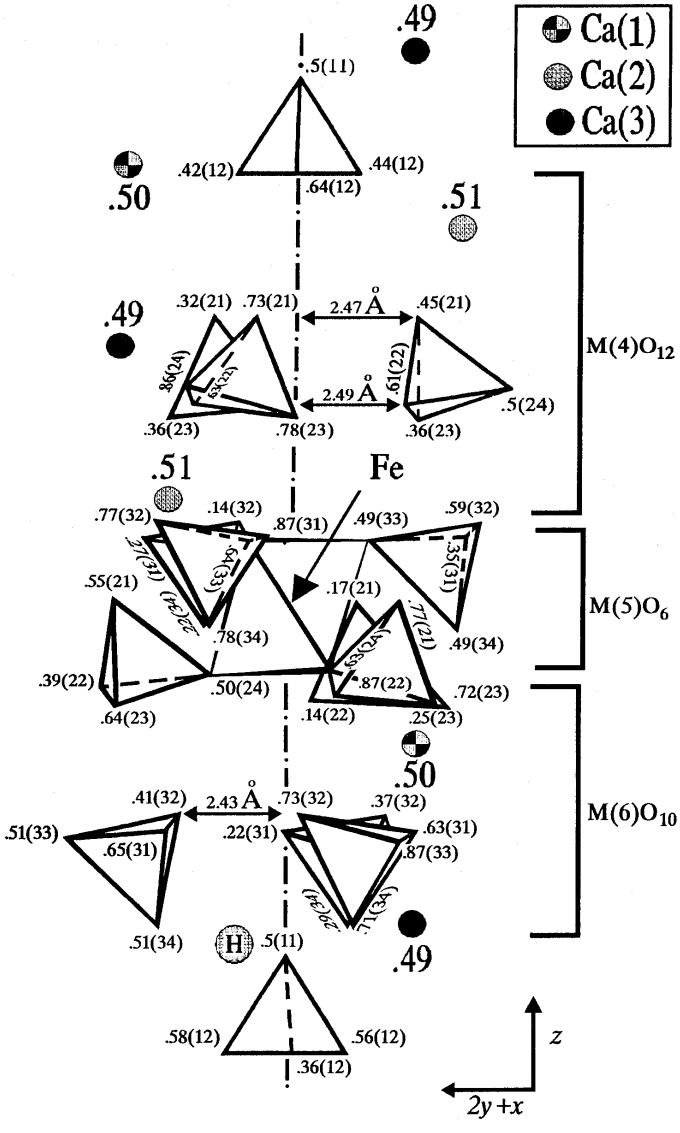

FIG. 4. A fragment of the structure of r-$Ca_9FeH_{0.9}(PO_4)_7$ showing $M(4)O_{12}$, FeO_6, and $M(6)O_{10}$ polyhedra. The figure indicates the atom heights along the X axis and their numbers (in brackets) in accordance with Table 2.

(6). Most experimental P–O, Ca–O, and Fe–O distances (Table 3) for the three structures are in good agreement with each other (within experimental errors). It is particularly true for s- and o-$Ca_9Fe(PO_4)_7$. However, the P(1)–O(11), P(2)–O(24), P(3)–O(33), and Fe–O(24) distances in the structure of r-$Ca_9FeH_{0.9}(PO_4)_7$ are different from the similar distances in the structures of s- and o-$Ca_9Fe(PO_4)_7$. The changes in the distances P(2)–O(24), P(3)–O(33), and Fe–O(24) are caused by the radius change of the iron cation ($r_{VI}(Fe^{2+})$ = 0.77 Å, $r_{VI}(Fe^{3+})$ = 0.645 Å) (17).

Each FeO_6 octahedron is linked to two different PO_4^{3-} groups. The octahedra in r-$Ca_9FeH_{0.9}(PO_4)_7$ are far more regular than those in s- and o-$Ca_9Fe(PO_4)_7$. The Fe–O(33) bond lengths are the same for s- and o-$Ca_9Fe(PO_4)_7$, and r-$Ca_9FeH_{0.9}(PO_4)_7$ but the Fe–O(24) (2.08 Å) bond distance in r-$Ca_9FeH_{0.9}(PO_4)_7$ is longer than the Fe–O(24) (1.96 Å, 1.95 Å) bond distances in s- and o-$Ca_9Fe(PO_4)_7$.

The position of hydrogen atoms was assumed proceeding from the study of the geometry of the structure, namely, mutual orientation of PO_4^{3-} tetrahedrons, intratetrahedral and intertetrahedral O–O distances, and empty polyhedra. The comparison of interatomic distances shows that there are two empty polyhedra $M(4)O_{12}$ and $M(6)O_{10}$ on the threefold crystallographic axis (Fig. 4). These polyhedra stretch along the threefold axis. The minimum distances X–O in these polyhedra are $d_{(X-O(21))}$ = 2.47 Å ($M(4)O_{12}$) and $d_{(X-O(32))}$ = 2.43 Å ($M(6)O_{10}$). In the widest sites of the polyhedra it is possible to place cations with the radius up to 1.4 Å, for example, Li^+, Na^+, K^+ (18), or protons. The comparison of distances in these polyhedra shows that protons can only be distributed in $M(6)O_{10}$ polyhedron.

The PO_4^{3-} tetrahedra in these three compounds are isolated like PO_4^{3-} groups in other whitlockite-like phosphates (6, 8–11). The P(1)–O(11) bond distance in r-$Ca_9FeH_{0.9}(PO_4)_7$ is 1.71(4) Å while s- and o-$Ca_9Fe(PO_4)_7$ have shorter P(1)–O(11) bond distances (1.62(4) and 1.56(3) Å). The long distances are similar to those reported for related compounds such as $Ca_{18}Mg_2H_2(PO_4)_{14}$ (8), $Ca_{18}Mn_2H_2(PO_4)_{14}$ (9), and mineral $Ca_{18.19}(Mg_{1.17}Fe_{0.83})H_{1.62}(PO_4)_{14}$ (6). The increase of the P(1)–O(11) distance can be connected with the formation of the O(11)–H hydrogen bond (Fig. 4). From the long H … O distance, it may be concluded that the bond is weak and may be realized with the O(34) oxygen atom. The distance O(11)–O(34) in r-$Ca_9FeH_{0.9}(PO_4)_7$ (2.57 Å) is noticeably decreased in comparison with s- (2.61 Å) and o-$Ca_9Fe(PO_4)_7$ (2.65 Å).

The hydrogen atoms in the structure form O(11)–H and O(34) … H bonds. The fine structures of the PO_4^{3-} groups for s- and o-$Ca_9Fe(PO_4)_7$ indicate a lower order point symmetry of the PO_4^{3-} ions and of their ionic environment in the lattice of r-$Ca_9FeH_{0.9}(PO_4)_7$. Descent of PO_4^{3-} group symmetry is explained by the fact that there are P–O–Ca, P–O–Fe, and P–O–H bonds in r-$Ca_9FeH_{0.9}(PO_4)_7$ while in phases s- and o-$Ca_9Fe(PO_4)_7$ there are only P–O–Ca and P–O–Fe bonds.

Thus, the experimental data prove that redox reactions in double calcium and iron phosphates proceed reversibly without destruction of the crystal lattice. The oxygen stoichiometry is not variable in these compounds. Apparently, similar reactions will proceed in solid solutions of $Ca_{3-x}Fe_{2x/3}(PO_4)_2$ that have been found in the $Ca_3(PO_4)_2$–$FePO_4$ system (19).

ACKNOWLEDGMENTS

The authors acknowledge support of the research by the International Science Foundation under Grant NBK 000 and the International Center for Diffraction Data (ICDD) under Grant-in-Aid 93-08.

REFERENCES

1. B. I. Lazoryak, V. A. Morozov, and M. S. Safonov, *Mater. Res. Bull.* **30,** 1269 (1995).
2. B. I. Lazoryak, P. Salmon, K. Parent, P. Hagenmuller, B. N. Viting, and A. B. Yaroslavzev, *Sov. Vestn. Mosc. Univ. Ser. 2 Khim.* **31,** 406 (1990).
3. B. I. Lazoryak, *in* "Fundamental Study of New Materials and Processes in the Substance," p. 54, Moscow Univ. Press, Moscow, 1994.
4. S. Attaly, B. Vigouroux, M. Lenzi, and J. Persia, *J. Catal.* **63,** 456 (1980).
5. R. Guardia-Useche, J. Lenzi, and M. Lenzi, *Bull. Soc. Chim. France* **1–2,** I-25 (1982).
6. C. Calvo, R. Gopal, *Am. Mineral.* **60,** 120 (1975).
7. M. S. Safonov, B. I. Lazoryak, S. B. Pozharskii, and S. B. Daschkov, *Rus. Dokl. Acad. Nauk* **338,** 633 (1994).
8. R. Gopal, C. Calvo, J. Ito, and W. K. Sabine, *Can. J. Chem.* **52,** 155 (1974).
9. E. Kostiner and J. R. Rea, *Acta Crystallogr.* **32,** 250 (1976).
10. B. Dickens, L. W. Schroeder, and W. E. Brown, *J. Solid State Chem.* **10,** 232 (1974).
11. L. W. Schroeder, B. Dickens, and W. E. Brown, *J. Solid State Chem.* **22,** 253 (1977).
12. S. Yu. Oralkov, B. I. Lazoryak, and R. G. Aziev. *Sov. J. Inorg. Chem.* **33,** 73 (1988).
13. H. M. Rietveld, *Acta Crystallogr.* **22,** 151 (1967).
14. F. Izumi, *J. Crystallogr. Sov. Jpn.* **27,** 23 (1985).
15. G. N. Kustova, E. N. Jurchenko, E. B. Burgina, M. M. Andruschkevich, and R. A. Buynov, *Soc. J. Struct. Chem.* **20,** 1019 (1979).
16. T. R. Narayanan Kutty, *Ind. J. Chem.* **8,** 655 (1970).
17. R. D. Shannon, *Acta Crystallogr. Sect. A* **32,** 751 (1976).
18. B. I. Lazoryak, S. V. Khoina, V. N. Golubev, and R. G. Aziev, *Sov. J. Inorg. Chem.* **35,** 1373 (1990).
19. B. I. Lazoryak, S. Yu. Oralkov, V. N. Golubev, and A. N. Zhdanova, *Sov. J. Inorg. Chem.* **34,** 1710 (1989).